Research Article

Photo-catalytic studies of Mn and Fe tetraphenyl porphyrins in the degradation of Amido Black 10B dye with solar light

S. D. Gokakakar[2] · P. A. Pavaskar[1] · A. V. Salker[1]

Received: 19 October 2019 / Accepted: 6 January 2020 / Published online: 30 January 2020

Abstract
The free base tetraphenyl porphyrin (TPP) and its metalloporphyrins such as tetraphenylporphinatomanganese chloride (MnTPPCl), μ-Oxo-bis [tetraphenylporphinatomanganese [O-$(MnTPP)_2$], tetraphenylporphinatoiron chloride (FeTPPCl) and μ-Oxo-bis [tetraphenylporphinatoiron] [O-$(FeTPP)_2$] were synthesized in the laboratory and characterized by UV–visible, IR, Proton NMR and Fluorescence spectroscopy. Diffused reflectance spectroscopy revealed that all these compounds are low band gap semiconducting type materials. The photo-degradations of Amido Black 10B were performed to explore the photo-catalytic activity of these porphyrins using solar radiation at different pH conditions. In the present experiment attempts were made to use metal porphyrins without any supporting material, indirectly also to prove the photodynamic capabilities of these materials. It was revealed that pH plays an important role in the degradation of dye. The HPLC analysis of the product showed three components with same retention time irrespective of pH and ion chromatography indicated the mineralization of dye during degradation process. The results have shown the mineralization of the dye by redox reactions that are taking place at the respective groups present in the dye molecule. This eco-friendly remediation appears as a promising technique for degradation or mineralization of organic matter from contaminated water resources.

Keywords Tetraphenyl porphyrin · Metalloporphyrins · Amido Black 10B · Ion-chromatography · Photocatalytic activity

1 Introduction

It is well known fact that industrial and textile dyes are continuously discharged intensive aromatic color wastes with high toxicity and often carcinogenic in nature. These dyes are also responsible for serious water pollution and percolation of such wastes into underground water sources causing a serious problem to the natural water resources. As far as current legislation regarding wastewater is concerned, it is mandatory on part of the concerned industry to treat this effluent by physical, chemical or biological methods before it is discharged into the respective sinks [1, 2]. Among the variety dyes used by the various industries, the azo dyes constitute nearly 60–70%. During the course of production and application, about 10% of them are lost in the form of colored effluent wastes [3]. It is a frequently observed that some azo dyes are oxidized aerobically. Nevertheless, sometimes they are degraded anaerobically, giving aromatic amines followed by further aerobic degradation [4]. In azo dyes, removal of color is possible only after the destruction of chromophoric structure. Their solubility in water are increased by presence of sulfonic acid group, which plays a role of auxochrome. Thus, due to large amount of organic compounds present in the dyes and their stability, modern dyes cannot be treated by conventional biological methods [5–7]. Besides

Electronic supplementary material The online version of this article (https://doi.org/10.1007/s42452-020-1989-8) contains supplementary material, which is available to authorized users.

✉ A. V. Salker, sal_arun@rediffmail.com; sav@unigoa.ac.in | [1]School of Chemical Sciences, Goa University, Taleigao, Goa 403 206, India. [2]P. E. S. S. R. S. N. College of Arts and Science, Farmagudi, Goa, India.

biological treatments, it is cost expensive with limited range of applicability.

In order to overcome above difficulties, heterogeneous photo-catalysis with semiconducting materials like TiO_2, ZnO, CdS etc. being used by different research workers [8]. Many researchers used mercury lamp, fluorescent lamp and halogen lamp to degrade the dye solution [9–11]. Further, the attempt is made to use naturally available solar radiation and observed that it is an effective source for the degradation processes, which can be applied to the wide range of the dyes [12–14]. In tropical countries, solar radiation is abundant and freely available for more than 8 months therefore, solar energy can be utilized to carry out photo-degradation of the azo dyes. TiO_2 is active only in ultraviolet portion of the solar spectrum. As a consequence the significant efforts have been made to develop modified forms of TiO_2 that are active in visible region (> 400 nm) by doping with suitable metal ions and functionalizing TiO_2 with photo-sensitizers that absorb visible-light [15–20].

In the recent past, it is a well-established fact that synthetic porphyrins are important because they are structurally related to biologically important compounds like heme, chlorophyll, cytochrome, vitamin B_{12} etc. Among their various versatile properties such as radiation sensitizers or protecting agents against radiations, they are also active elements of biosensors, elements of selective electrodes and non-linear optical materials [21, 22]. Further, photo-catalytic properties of synthetic porphyrins [23, 24], their role as pigments and dyes, semiconductors, analytical reagents and photodynamic therapy have proved their indispensability in the scientific domain.

The present objective of photo-degradation of Amido Black 10B emphasizes the use of self-synthesized tetraphenyl porphyrin, monomer and dimers of metalloporphyrins in pure form containing Mn and Fe metals. As discussed above that the few research workers have used porphyrins, which were supported on TiO_2 or any other suitable inorganic photo-catalyst, to carry out photo-degradation in the visible region. However, in the present studies, attempts are made to use porphyrins without any supporting material, indirectly also to prove the photodynamic capabilities of these materials. Prior to use as photo-catalysts, their thermal stability measurements are carried out and it is found that they are quite stable up to 400 °C [25]. It is further investigated the co-relationship between photo-degradation activity of porphyrins with fluorescence exhibited by the respective metalloporphyrins. The simple reaction assembly was designed for photo-degradation. The use of oxidizing agents such as hydrogen peroxide (H_2O_2) or potassium per sulfate ($k_2S_2O_8$) was purposely avoided to verify the efficiency of the reaction. The reaction mixture was stirred with a time interval of 10 min. In addition to this, complete degradation of Amido Black 10B was verified with HPLC and quantitative estimation of mineralized cations and anions was done by ion-chromatography.

2 Methodology

2.1 Synthesis of TPP

The free-based TPP was synthesized by the established method [26]. An equimolar quantity of AR grade pyrrole and benzaldehyde were refluxed in propionic acid for half an hour. The assembly was cooled, filtered and washed with hot methanol followed by hot water. The shiny purple colored crystals of TPP were recovered and subjected to vacuum drying for removal of any remaining moisture. Further, this product was purified by dry column chromatography where silica gel was used as a stationary phase and $CHCl_3$ as mobile phase. The purity of TPP was checked using thin layer chromatography (TLC) where thin layer was comprised of petroleum ether and chloroform (80%: 20%).

2.2 Synthesis of metalloporphyrins

The monomers tetraphenyl-porphinatomanganese(III) chloride (MnTPPCl) and tetraphenylporphinato-iron(III) chloride (FeTPPCl) were synthesized [27] by adding the corresponding salt of the metal to refluxing solution of dimethyl formamide (DMF) containing TPP in stoichiometric proportion. The refluxing time for the reactions was modified to more than 1 h. The dimer of Mn i.e. µ-Oxo-bis [tetraphenylporphinato-manganese(III)] [O-$(MnTPP)_2$] was synthesized by dissolving purified MnTPPCl in pyridine and then 30% KOH was added. Then the reaction mixture was evaporated to dryness on a steam bath. The alkali was removed by washing the solid with water. This process was repeated for two times. The final dried product was recrystallized from benzene. The crystals were collected and dried in vacuum desiccators. The dimer µ-Oxo-bis [tetraphenylporphinato-iron(III)] [O-$(FeTPP)_2$] was synthesized using suitable method by dissolving purified FeTPPCl in $CHCl_3$ and adding 25% KOH and the solution was stirred for 1 h [28]. The chloroform layer was separated from water layer and further purified by dry column chromatography with silica gel as stationary phase and a mobile phase consisting of gradient mixture of chloroform and methanol (50%: 50%). TLC checked the purity of above metallo-porphyrins as above.

2.3 Characterization of porphyrins

UV–visible spectra were recorded using Shimadzu UV–visible spectrophotometer (model UV/2450 UV) for 10^{-4} M and 10^{-5} M concentrations for each porphyrin. Infrared analysis was carried out using Shimadzu FTIR spectrometer (model prestige/21 FTIR). Proton NMR spectra were recorded using Varian 300 MHz model. Fluorescence study for the samples was carried out using Shimadzu spectrofluorimeter (model RF-5301 PC). Diffused reflectance spectroscopy (DRS) study was performed to calculate band gap energies on Shimadzu UV–visible spectrophotometer (model UV/2450 UV).

2.4 Photo-degradation of Amido Black 10B

Solar assisted photo-catalytic degradations of azo dye Amido Black 10B were carried out using above synthesized free-based TPP, monomers and dimers of Mn and Fe during 11.30 a.m. to 3.30 p.m. in the afternoon. This heterogeneous photo-degradation process was then employed for the dye solution of 10^{-5} M concentration in aqueous media, which was pre–saturated with oxygen for 5 min at pH values of 6, 7 and 10 respectively. This mixture was placed in a closed glass reactor, which was kept in sunlight for the photo-degradation reaction. The mixture was stirred after every 10 min gap. The reaction was studied at different pH conditions. The degraded reaction mixtures at pH 6 and 7 were subjected to high performance liquid chromatography (HPLC) using Perkin Elmer SERIES-200 with C18 column of dimensions 250 × 4.6 mm and particle size 5 mm. The solvent system selected was methanol and water 80: 20% with UV detector, which functions at 254 nm. The degraded reaction mixture at pH 7 was then subjected to ion chromatography using cation and anion exchangers. Ion-chromatography using Shodex-CD 5 analyzer, did the qualitative and quantitative analysis of dye mineralization. The basic objective of these studies is to find the efficiency of dye degradation or mineralization efficiency by this process.

3 Results and discussion

3.1 UV–visible spectroscopy

The porphyrins TPP, MnTPPCl, [O-(MnTPP)$_2$], FeTPPCl and [O-(FeTPP)$_2$] were characterized by UV–visible spectroscopy. The absorption bands appearing for these compounds in the soret and visible region are in good agreement with the literature values and is shown in Table 1. In the above series, TPP is a free-base porphyrin where there is no metal and remaining metalloporphyrins are called hyper porphyrins due to the strong interaction between metal and porphyrin ring. The monomer MnTPPCl shows 376 nm and 425 nm absorption bands in soret region whereas these bands are absent in its dimer [O-(MnTPP)$_2$]. In the visible region, the band due to dimer [O-(MnTPP)$_2$] i.e. 527 nm is blue shifted in comparison with MnTPPCl band i.e. 582 nm. Similarly, dimer [O-(FeTPP)$_2$] shows blue shift in soret as well as in visible region in comparison with FeTPPCl. When the absorption bands of MnTPPCl and FeTPPCl are compared, it is seen that latter shows blue shift and when the dimers [O-(MnTPP)$_2$] and [O-(FeTPP)$_2$] are compared the same trend of slight blue shift is seen in the Fe-dimer. Figure 1 shows UV–Visible spectra of MnTPPCl for 10^{-4} M and 10^{-5} M concentrations where all bands are completely resolved for 10^{-5} M concentration.

Table 1 Absorption peaks in Soret and Q-bands

Porphyrin	Absorption bands				
	Soret band	←	Q-bands	→	
TPP	416	515	549	590	647
MnTPPCl	376	479		582	618
O-(MnTPP)$_2$	–	479	527	580	616
FeTPPCl	416	509		572	609
O-(FeTPP)$_2$	408			571	611

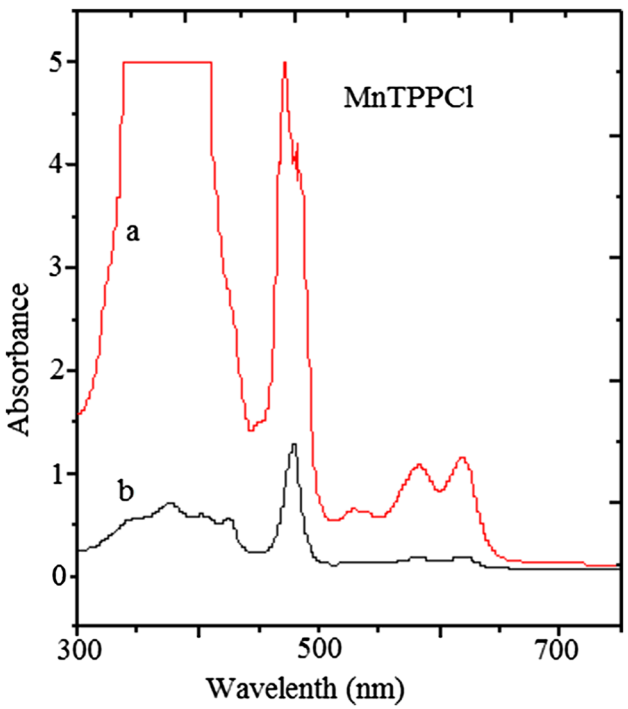

Fig. 1 UV–visible spectra of MnTPPCl (a) 10^{-4} M concentration, (b) 10^{-5} M concentration

3.2 Infrared spectroscopy

The above porphyrins show various absorption bands in infrared region of which some are characteristic for a given porphyrin. TPP shows medium N–H stretching vibrations at 3317 cm^{-1}. When a metal is inserted into a porphyrin ring this band disappears due to replacement of two acidic hydrogens by metal and further individual characteristic bands are developed. Therefore, IR is used for characterization of metalloporphyrins. Figure S1 (in supplementary) shows IR spectra of O-$(MnTPP)_2$ as a representative sample.

The strong absorption band near 1000 cm^{-1} appears due to vibration of the porphyrin ring or pyrrole units, which is sensitive to the nature of the metal ion. Further, it establishes the strength of the metal-nitrogen bonds in the TPP chelates. The Recorded IR spectra of all the above metalloporphyrins show that the strength of the metal-nitrogen bond is in the following order i.e., FeTPPCl < O-$(FeTPP)_2$ < MnTPPCl < O-$(MnTPP)_2$. The characteristic absorption bands for respective metalloporphyrins in the region 820–940 cm^{-1} are shown in Table 2. These frequencies are characteristic of the C–H rocking for the pyrrole rings of a particular porphyrin [28, 29].

3.3 Proton NMR spectroscopy

Proton NMR spectroscopy is used as characterization tool with reference to chemical shift, the splitting of absorption signals due to spin–spin interactions and the intensity of absorption signals. In the above synthesized porphyrins, MnTPPCl, O-$(MnTPP)_2$, FeTPPCl and O-$(FeTPP)_2$ are paramagnetic in nature, only TPP, a free-base porphyrin is diamagnetic. Further, as a representative compound of all synthesized paramagnetic metalloporphyrins, FeTPPCl shows following results. The chemical shift due to m-phenyl protons is 7.2 ppm, p-phenyl protons 6.4 ppm and peak due to β-pyrrole protons is 7.7 ppm respectively, which is shown in Fig. S2 (in supplementary).

Table 2 Infra red spectra, Band gap energies and Fluorescence intensities of TPP and metalloporphyrins

Porphyrin	Absorption bands (cm^{-1})	Band gap (eV)	Fluorescence intensity
TPP	850 (w)	1.75	14.69
MnTPPCl	833 (w)	1.70	56.72
O-$(MnTPP)_2$	867 (s)	1.69	46.06
FeTPPCl	834 (w)	1.71	2.88
O-$(FeTPP)_2$	878 (s)	1.58	2.71

3.4 Fluorescence spectroscopy

The fluorescence spectra of above synthesized porphyrins were recorded at an excitation wavelength of 420 nm. Among these, TPP, MnTPPCl, and O-$(MnTPP)_2$ were found fluorescent whereas FeTPPCl and O-$(FeTPP)_2$ were seen as non-fluorescent as shown in Table 2. The degree of fluorescence intensity of the respective fluorescent porphyrins is shown in Fig. 2, which are in the following order i.e. MnTPPCl > O-$(MnTPP)_2$ > TPP. Further, it was revealed that fluorescent porphyrins are effective photo-catalysts than non-fluorescent porphyrins in the photo-degradation process. The reason is that free-base porphyrins and other metalloporphyrins possess sharp and intense long wavelength electronic transitions with relatively long-lived excited states. This makes them ideal photo agents.

In porphyrins excited states are due to π–π^* transitions and they are not perturbed energetically due to the substitution of different metals. However, the different metals influence the life spans and luminescence properties of the porphyrins [30]. In above studies it is evident that even though fluorescence intensity of MnTPPCl is higher than remaining two such as O-$(MnTPP)_2$ and TPP, the long lived excited states would be more for these two than former one. This makes MnTPPCl relatively a weaker photo-catalyst than O-$(MnTPP)_2$ and TPP respectively.

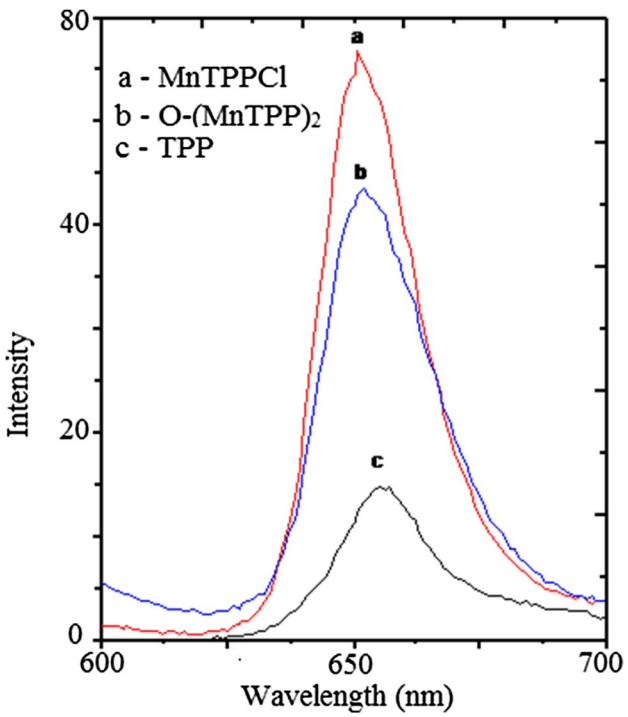

Fig. 2 Fluorescence spectra of TPP, MnTPPCl and O-$(MnTPP)_2$

3.5 Diffuse reflectance spectroscopy

The band gap energies of these porphyrins are calculated using diffused reflectance spectroscopy (DRS) as shown in Table 2. It is also seen that band gap energies range between 1.58 and 1.75 eV, which indicates that they are low band gap metal–organic semiconductors.

Further, it was felt interesting to employ these semiconductors for the photo-degradation of diazo dye like Amido Black 10B as a model reaction and subsequently assess their individual capacity as photo catalysts. Since porphyrins are chromophoric pigments which impart them very strong intense colour, therefore, the DRS spectra of solid powders show some absorption peaks which match with the absorption peaks in solution form with some shifts in λ values [31, 32]. Figures S3 and S4 (in supplementary) show DRS spectra of MnTPPCl and O-$(MnTPP)_2$ as representative samples.

3.6 Photo-degradation process

Photo-degradation of Amido Black 10B was carried out using solid powders of TPP, MnTPPCl, O-$(MnTPP)_2$, FeTPPCl and O-$(FeTPP)_2$ as heterogeneous photo-catalysts in the glass reactor. The visible spectrum of Amido Black 10B at pH 6, 7 and 10 is found to be $\lambda_{max} = 618$ nm in aqueous media. The progress of the photo-degradation process is examined by measuring the absorbance at above-mentioned wavelength with time interval of 1, 2, 3 and 4 h respectively. For above degradation process the optimum conditions are used by taking into account the different parameters such as absence of catalyst, presence of catalyst with specific amount, saturating reaction mixture with O_2 and without O_2, time of irradiation, use of surfactants as promoters and different conditions of pH at 6, 7, and 10 respectively. This is to measure the efficiency of activity for degradation or removal of dye at different time intervals.

3.7 Amount of catalyst

The optimum amount of photo-catalyst was determined by varying the amount of porphyrins and recording the corresponding absorbance for a 100 mL of 10^{-5} M dye solution. Therefore, the amount of photo-catalyst in mg was varied from 5, 10, 15, 20, 25, 30, 35, and 40 respectively. Further, it was found that for 25 mg of photo-catalyst the minimum absorbance or maximum degradation was seen under ideal conditions and therefore, this amount was fixed for all photo-catalytic reactions. It was also observed that when the amount exceeded 25 mg, the efficiency of degradation is reduced. The reason for this may be attributed to that when the amount of photo-catalyst is more than optimum quantity then the rate of deactivation of activated molecules increases due to collision with ground state molecules hence reduction in activity of the photo-catalysts [33, 34].

3.8 Reaction assembly

By examining all the ideal possibilities for effective photo-degradation with due emphasis with respect to above parameters following reaction assembly was prepared. In a simple glass reactor or simple conical flasks of 150 ml capacity were used, 100 mL of 10^{-5} M dye solution was saturated with O_2 for 5 min and loaded with 25 mg of respective photo-catalyst; the solution was stirred and kept in sunlight always between 11.30 a.m. to 3.30 p.m. The solution was intermittently stirred with a gap of 10 min.

3.9 Photo-degradation at different pH

The above-mentioned synthesized porphyrins were used as photo-catalysts for the degradation of Amido Black 10B at pH 6, 7, and 10 as shown in Figs. 3, 4 and 5 respectively. As per the observations, it is seen that photo-catalytic activity is maximum at pH 6, good for pH 10 and minimum at pH 7. The concerned photo-degradations were carried out for 1–4 h with solar radiations during above-mentioned time. At pH 6, it is seen that, O-$(MnTPP)_2$ and TPP showed 100% degradation of the dye, MnTPPCl showed nearly 90% whereas O-$(FeTPP)_2$ and FeTPPCl gave 36% and

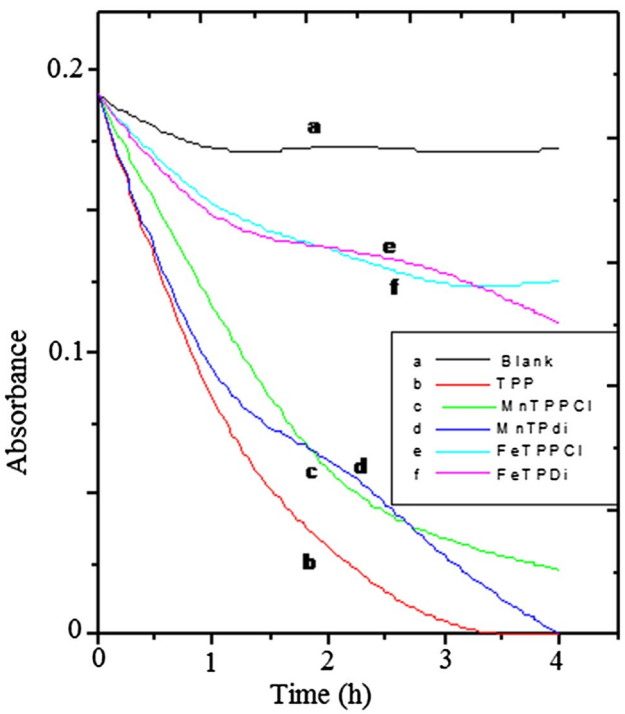

Fig. 3 Photocatalytic degradation of Amido Black 10B at pH 6

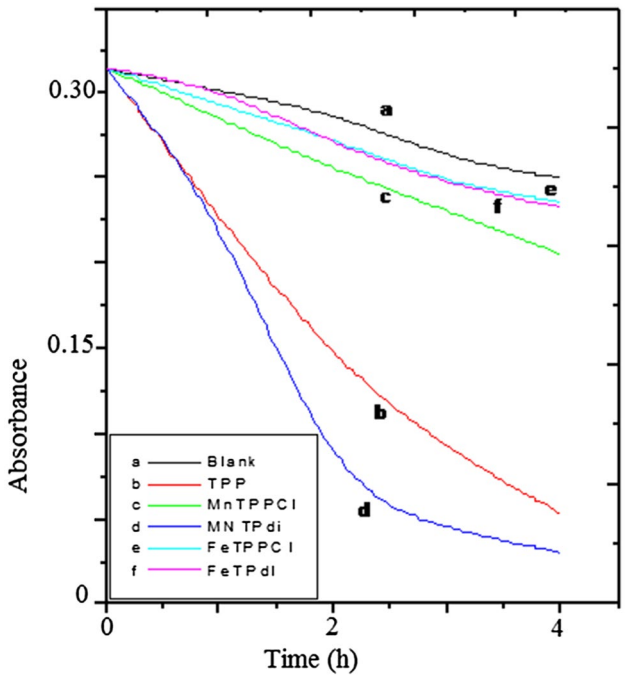

Fig. 4 Photocatalytic degradation of Amido Black 10B at pH 10

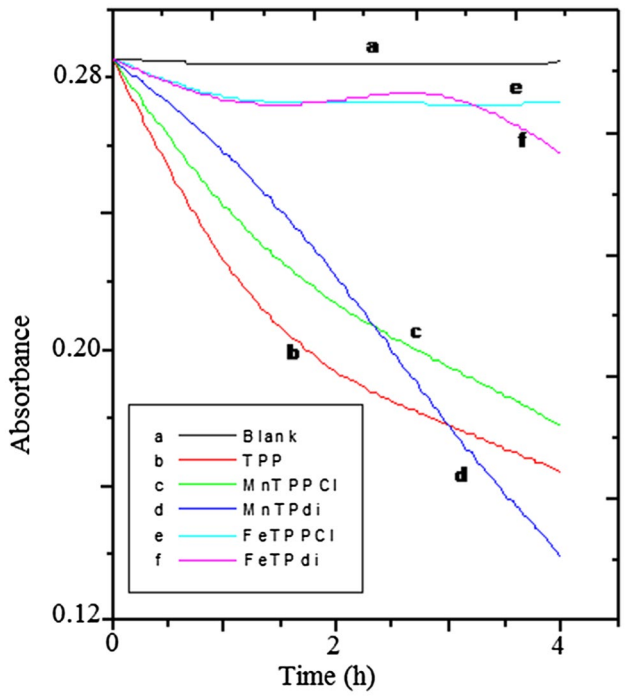

Fig. 5 Photocatalytic degradation of Amido Black 10B at pH 7

28% degradation respectively as seen in Fig. 3. For pH 10, O-$(MnTPP)_2$ showed 90% degradation, TPP—81%, MnTPPCl—32%, O-$(FeTPP)_2$—25% and FeTPPCl—23% (Fig. 4). At pH 7, O-$(MnTPP)_2$ gave 54% degradation, TPP—45%, MnTPPCl—40%, O-$(FeTPP)_2$—13% and FeTPPCl—10% respectively (Fig. 5). The blank solution at pH 10 showed little degradation, might be due to the presence of OH^- ions, which are responsible for the production of $OH^\bullet$ radicals and further degradation of the dye. At pH 7, the activity of dye was low, therefore, five drops of 0.1% of sodium lauryl sulphate (SLS) was added as promoter whereby photocatalytic activity enhanced comparatively in the same order. Since at pH 6 showed maximum efficiency indicates that the H^+ ions may be beneficial in the formation of $OH^\bullet$ radicals which are responsible for photo-degradation on these catalysts. In spite of higher fluorescence in MnTPPCl showed little lower activity than other fluorescent compounds. This is due to MnTPPCl contains chloride which normally suppresses the catalytic activity.

Thus it is seen that at pH 6, 10 and 7, O-$(MnTPP)_2$, TPP and MnTPPCl are the most effective photo-catalysts whereas O-$(FeTPP)_2$ and FeTPPCl showed low photocatalytic activity. The reason may be attributed to the fact that O-$(MnTPP)_2$, TPP and MnTPPCl are fluorescent porphyrins whereas O-$(FeTPP)_2$ and FeTPPCl are non-fluorescent metalloporphyrins. Since, fluorescence intensity is directly proportional to the amount of solar radiation absorbed; therefore, these photo-catalysts are effective as there is a constant and steady supply of longer wavelength solar radiation required for the dye degradation process. Among them O-$(MnTPP)_2$ and TPP are the superior because they would be maintaining comparatively more long-lived excited states as compared to MnTPPCl. Figure 6 shows the photo-degradation of Amido Black 10B at pH 6 by O-$(MnTPP)_2$ with time. Further, to check the reproducibility of the photo-catalytic activity, TPP as a representative sample was recycled for three times. It was observed that it's catalytic activity decreases for the second cycle and remains constant for next cycle. It was also observed that there is no change in the chemical composition of the photo-catalysts after photo-degradation reaction that was confirmed by UV–Visible and IR spectroscopy.

3.10 HPLC analysis

HPLC analyzer containing C-18 column was used to know the number of components, if any, are present in the un-degraded and degraded solution of Amido Black 10B at pH 6 and 7 respectively as shown in Fig. 7. It is seen that un-degraded solution of the dye does not show presence of any components. On the other hand, it is seen that at pH 6, the degraded solution shows three components, which are in very small amount and are separated at the retention time 3.37, 3.57 and 7.04 s respectively. Similarly, at pH 7, the retention time observed for the three components of the degraded dye solution was 3.37, 3.61 and 7.17 s respectively. Thus, it can be concluded that irrespective

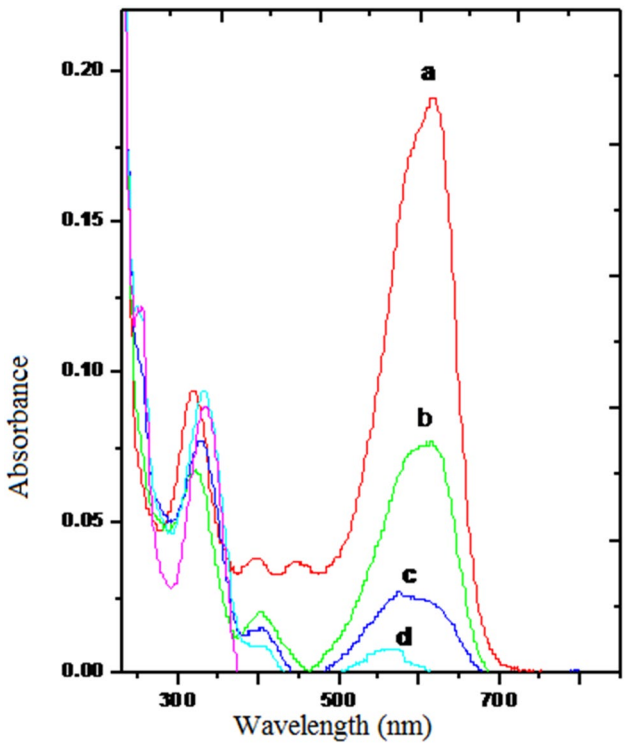

Fig. 6 Photocatalytic degradation of Amido Black 10B at pH 6 by O-$(MnTPP)_2$ with time (a) after 1 h, (b) 2 h, (c) 3 h and (d) 4 h

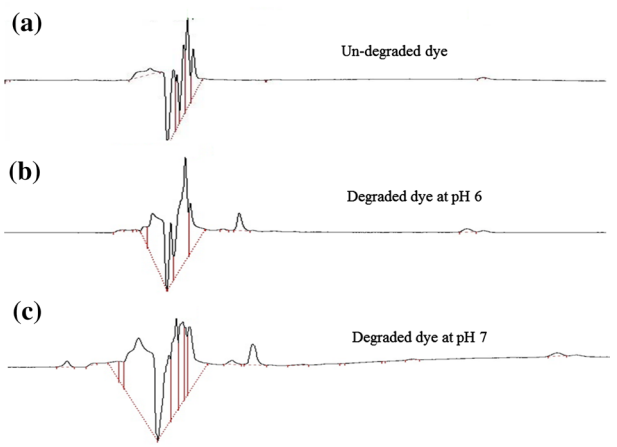

Fig. 7 HPLC results showing **a** undegraded Amido Black 10B solution, **b** degraded solution of Amido Black 10B at pH = 6, **c** degraded solution of Amido Black 10B at pH = 7

pH of the solution, the identical components are separated in a photo-catalytic reaction solution.

3.11 Ion-chromatography analysis

The qualitative and quantitative study of mineralization of the dye was carried out using ion-chromatography with Shodex-CD 5 analyzer. From the knowledge of the structure of Amido Black 10B, the cation analyzer was calibrated for the presence of Na^+ and NH_4^+ ions whereas anion analyzer was calibrated for NO_2^-, NO_3^- and SO_4^{2-} ions respectively. Figure 8 show cation-chromatograms for un-degraded (A) and degraded dye solutions (B) at pH = 7. It is also seen that un-degraded solution contains small amount of Na^+ ions i.e. 1.41 µg/mL which can be compared with amount of Na^+ in degraded solution which is 11.29 µg/mL. Similarly NH_4^+ ions are absent in the un-degraded solution and the amount of NH_4^+ ions in degraded solution was found to be 0.59 µg/mL. Figure 9 shows anion-chromatograms for un-degraded (A) and degraded solutions of the dye (B) at pH = 7. It is seen that very small amounts of NO_3^- (2.11 µg/mL) and SO_4^{2-} (0.50 µg/mL) are present in degraded solution. The above information is summarized in Table 3. These results reveal that during the process of photo-catalytic reaction along with the destruction of the azo groups of Amido Black 10B, a process of mineralization has taken place where possible inorganic ions are present on the microgram level. Similarly, it is seen that NH_2 group is reduced to NH_4^+ and NO_2^- and SO_3^{2-} groups are oxidized to NO_3^- and SO_4^{2-} respectively. Thus, redox reactions are seen to be taking place at the respective groups present in the Amido Black 10B molecule.

3.12 Mechanism of photo-catalytic reaction

It is well-evidenced fact that for the degradation of the dye, destruction of azo group is required. In general, decolorization rates of the dyes are different due to the complicated chemical structures containing polyatomic and sulfonate groups. Similarly, azo compounds with hydroxyl groups or with amino groups are more likely to be degraded at faster rates than those with methyl, methoxy sulfo or nitro groups [35]. By exposing to solar radiations, metal porphyrin semiconductors will be excited by light to give excited state porphyrins. This excited state will generate electron (e^-) in conduction band leaving hole (h^+) in the valence band. This e^- is then trapped by molecular O_2 forming O_2^- ions. The valence band h^+ generates hydroxyl radicals ($OH^{\cdot}$) from OH^- ions. These hydroxyl radicals readily attack the adsorbed dye, leading to degradation. It is a well-documented fact that hydroxyl radicals are responsible for the degradation of the dye since they are highly reactive and non-specific oxidant with an oxidation potential of 2.8 eV. Due to their very short life span (70 ns), they attack immediately in their vicinity, especially at the

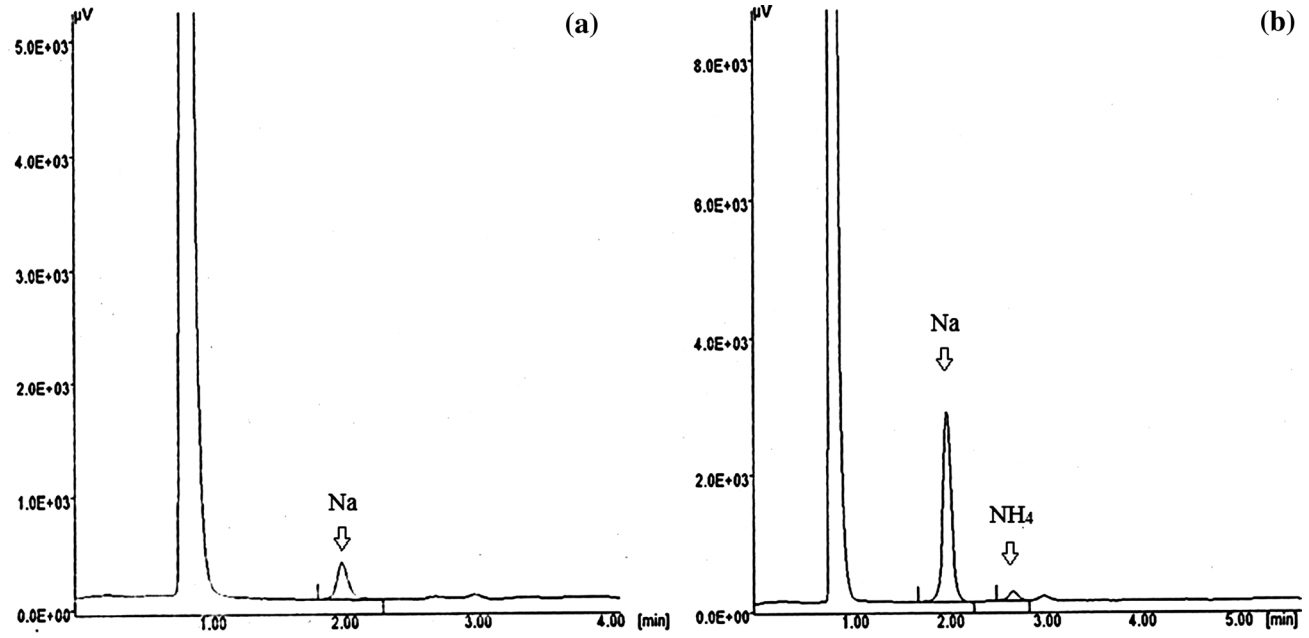

Fig. 8 Ion-chromatography results for cation analysis at pH = 7 **a** undegraded Amido Black 10B solution, **b** degraded Amido Black 10B solution

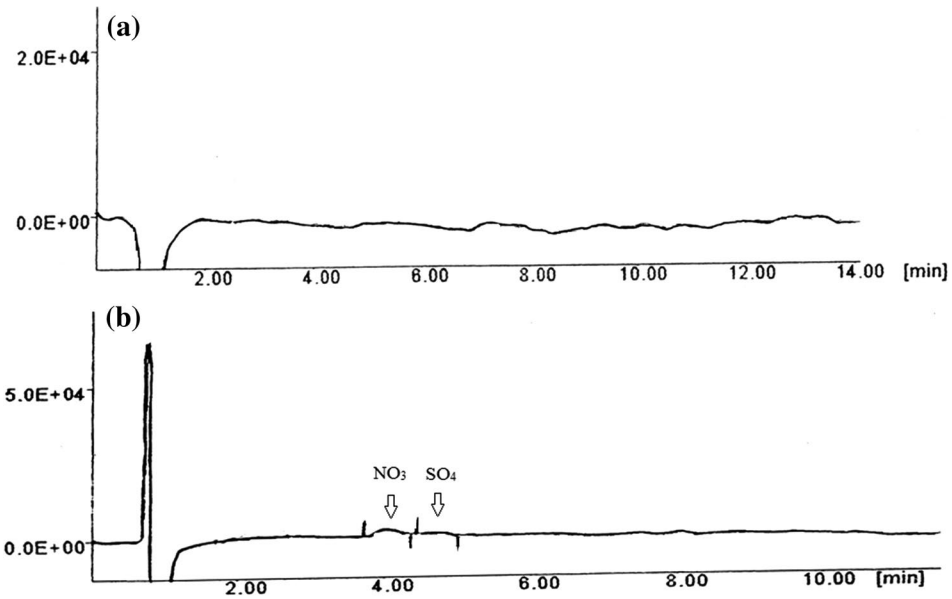

Fig. 9 Ion-chromatography results for anion analysis at pH = 7 **a** undegraded Amido Black 10B solution, **b** degraded Amido Black 10B solution

Table 3 Ion-chromatography results

Parameter	Undeg Na^+	Deg Na^+	Undeg NH_4^+	Deg NH_4^+	Undeg NO_3^-	Deg NO_3^-	Undeg SO_4^{2-}	Deg SO_4^{2-}
Conc. (μg/mL)	1.41	11.29	–	0.59	–	2.11	–	0.50
Retention time (min)	2.017	2.017	–	2.708	–	4.025	–	4.683
Peak area (μV s)	1950.5	16,497.6	–	846.2	–	27,934.4	–	9301.5

Undg undegraded dye solution, *Deg* degraded dye solution

π-bonds in the azo groups [36–38]. This is similar to Langmuir- Hishelwood type model in which require asorbed state of hydroxyl radicals and dye on the active sites near the porphyrin semiconductor catalyst for the redox reaction to take place for degradation. Further, it was proposed that this degradation process passes through the plausible mechanisms such as radical de-nitration, radical desulfonation and formation of keto-imine [39]. Thus, the degradation process of the dye seems to be complicated and various intermediate products are involved in it.

4 Conclusion

The monomers and dimers of manganese and iron tetra phenyl porphyrins were synthesized and purified by modified dry column chromatography. They were characterized by UV–visible spectroscopy, IR spectroscopy, NMR spectroscopy and fluorescence spectroscopy. Their semiconducting property was confirmed by Diffused Reflectance spectroscopy and used for degradation of Amido Black 10B at pH 6, 7 and 10 respectively. It was also observed that degradation of the dye is maximum at pH 6, good at pH 10 and low at pH 7. Further, it is seen that fluorescent photo-catalysts such as (TPP) and its metalloporphyrins such as O-$(MnTPP)_2$, MnTPPCl are efficient than non-fluorescent O-$(FeTPP)_2$ and FeTPPCl compounds. HPLC results have shown that in degraded dye solutions at pH 6 and 7 there are three products of very low concentration with nearly same retention time, which confirm the same reaction products are formed irrespective of the pH of degraded solution. Ion-chromatography results have shown the mineralization of the dye into Na^+, NH_4^+ (reduction product), NO_3^- and SO_4^{2-} (oxidation products) as a part of the degradation process. This indicates that redox reactions are taking place at the respective groups present in the dye molecule.

Acknowledgements Authors are grateful to UGC - New Delhi for the financial support.

Compliance with ethical standards

Conflict of interest The authors declare no conflict of interest.

References

1. Robinson T, Mcmullan G, Marchant R, Nigam P (2001) Remediation of dyes in textile effuent: a critical review on current treatment technologies with a proposed alternative. Bioresour Technol 77:247–255
2. Kannan N, Meenakshisundaram M (2002) Adsorption of congo red on various activated carbons a comparative study. Water Air Soil Pollut 138:289–305
3. Sökmen M, Allen DW, Akkas F et al (2001) Photo-degradation of some dyes using Ag-loaded titanium dioxide. Water Air Soil Pollut 132:153–163
4. Azmi W, Sani RK, Banerjee UC (1998) Biodegradation of triphenylmethane dyes. Enzyme Microb Technol 22:185–191
5. Balcioglu IA, Arslan I (2010) Treatment of textile waste water by heterogenous photocatalytic oxidation processes. Environ Technol 18:1053–1059
6. Arslan I, Balcioglu IA, Tuhkanen T, Bahnemann D (2000) H_2O_2/UV-C and Fe^{2+}/H_2O_2/UV-C versus TiO_2/UV-A treatment For reactive dye wastewater. J Environ Eng 126:903–911
7. Stock NL, Peller J, Vinodgopal K, Kamat PV (2000) Combinative sonolysis and photocatalysis for textile dye degradation. Environ Sci Technol 34:1747–1750
8. Neppolian B, Choi HC, Sakthivel S et al (2002) Solar/UV-induced photocatalytic degradation of three commercial textile dyes. J Hazard Mater 89:303–317
9. Arslan I, Akmehmet I, Bahnemann DW (2002) Advanced oxidation of a reactive dyebath effluent: comparison of O_3, H_2O_2/UV-C and TiO_2/UV-A processes. Water Res 36:1143–1154
10. Wang G, Liao C-H, Wu F-J (2001) Photodegradation of humic acids in the presence of hydrogen peroxide. Chemosphere 42:379–387
11. Rashed MN, El-Amin AA (2007) Photocatalytic degradation of methyl orange in aqueous TiO_2 under different solar irradiation sources. Int J Phys Sci 2:73–81
12. Vinodgopal K, Wqynkoop DE (1996) Environmental photochemistry on semiconductor surfaces: photosensitized degradation of a textile Azo Dye, Acid Orange 7, on TiO_2 particles using visible. Environ Sci Technol 30:1660–1666
13. Zhang F, Zhaoa J, Shen T et al (1998) TiO_2-assisted photodegradation of dye pollutants II. Adsorption and degradation kinetics of eosin in TiO_2 dispersions under visible light irradiation. Appl Catal B Environ 15:147–156
14. Epling GA, Lin C (2002) Photoassisted bleaching of dyes utilizing TiO_2 and visible light. Chemosphere 46:561–570
15. Mrowetz M, Balcerski W, Colussi AJ et al (2004) Oxidative power of nitrogen-doped TiO_2 photocatalysts under visible illumination. J Phys Chem B 108:17269–17273
16. Teoh WY, Amal R, Madler L, Pratsinis SE (2007) Flame sprayed visible light-active Fe–TiO_2 for photomineralisation of oxalic acid. Catal Today 120:203–213
17. Zhang X, Lei L (2008) One step preparation of visible-light responsive Fe–TiO_2 coating photocatalysts by MOCVD. Mater Lett 62:895–897
18. Kim S (2006) Photocatalytic activity of Ni 8 wt%-Doped TiO_2 photocatalyst synthesized by mechanical alloying under visible light. J Am Ceram Soc 89:515–518
19. Park H, Choi Wonyong, Hoffmann MR (2008) Effects of the preparation method of the ternary CdS/TiO_2/Pt hybrid photocatalysts on visible light-induced hydrogen production †. J Mater Chem 18:2379–2385
20. Bae E, Choi W (2003) Highly enhanced photoreductive degradation of perchlorinated compounds on dye-sensitized metal/TiO_2 under visible light. Environ Sci Technol 37:147–152
21. Datta-Gupta N, Bardos TJ (1966) Synthetic porphyrins. I. Synthesis and spectra of some para-substituted meso-tetraphenylporphines. J Heterocycl Chem 3:495–502
22. Milgrom LR (1997) The colours of life: an introduction to the chemistry of porphyrins and related compounds. In: The

colours of life: an introduction to the chemistry of porphyrins and related compounds. Oxford University Press, Oxford
23. Salker AV, Gokakakar SD (2009) Solar assisted photo-catalytic degradation of Amido Black 10B over cobalt, nickel and zinc metalloporphyrins. Int J Phys Sci 4:377–384
24. Gokakakar SD, Salker AV (2009) Solar assisted photocatalytic degradation of methyl orange over synthesized copper, silver and tin metalloporphyrins. Indian J Chem Technol 16:492–498
25. Gokakakar SD, Salker AV (2010) In: Proceedings of 17th National Symposium. In: Thermans, pp 282–283
26. Adler AD, Longo FR, Finarelli JD et al (1966) A simplified synthesis for meso-tetraphenylporphin. J Org Chem 32:476
27. Adler AD, Longo FR, Kampas F, Kim J (1970) On the preparation of metailoporphyrins. J Inorg Nucl Chem 32:2443–2445
28. Fleischer EB, Palmer JM, Srivastava TS, Chatterjee A (1971) Thermodynamic and kinetic properties of an iron-porphyrin system. J Am Chem Soc 93:3162–3167
29. Thomas DW, Martell AE (1959) Metal chelates of tetraphenylporphine and of some p-substituted derivatives. J Am Chem Soc 81:5111–5119
30. Hoff FR, Whitten DG (1978) The volume II structure and synthesis. In: Dolphin D (ed), 2nd edn. Acadamic press, pp 161–162
31. Özgür Ü, Alivov YI, Liu C et al (2005) A comprehensive review of ZnO materials and devices. J Appl Phys 98:41301
32. Aoki T, Hatanaka Y, Look DC (2000) ZnO diode fabricated by excimer-laser doping ZnO diode fabricated by excimer-laser doping. Appl Phys Lett 76:3257–3258
33. Sakthivel S, Geissen S, Bahnemann DW et al (2002) Enhancement of photocatalytic activity by semiconductor heterojunctions: alpha-Fe_2O_3, WO3 and CdS deposited on ZnO. J Photochem Photobiol 148:283–293
34. Borker P, Salker AV (2006) Photocatalytic degradation of textile azo dye over $Ce_{1-x}Sn_xO_2$ series. Mater Sci Eng 133:55–60
35. Poonam N, Banat IM, Singh D, Marchanv R (1996) Microbial process for the decolorization of textile effluent containing Azo, Diazo and reactive dyes. Process Biochem 31:435–442
36. Karkmaz M, Puzenat E, Guillard C, Herrmann JM (2004) Photocatalytic degradation of the alimentary azo dye amaranth Mineralization of the azo group to nitrogen. Appl Catal B Environ 51:183–194
37. Chen T, Zheng Y, Lin J-M, Chena G (2008) Study on the photocatalytic degradation of Methyl Orange in water using Ag/ZnO as catalyst by liquid chromatography electrospray ionization ion-trap mass spectrometry. J Am Soc Mass Spectrom 19:997–1003
38. Erdemoglu S, Aksu SK, Sayılkan F et al (2008) Photocatalytic degradation of Congo Red by hydrothermally synthesized nanocrystalline TiO_2 and identification of degradation products by LC–MS. J Hazard Mater 155:469–476
39. Meetani MA, Hisaindee SM, Abdullah F et al (2010) Chemosphere Liquid chromatography tandem mass spectrometry analysis of photodegradation of a diazo compound: a mechanistic study. Chemosphere 80:422–427